Folding model analysis of proton scattering from ^{18,20,22}O nuclei

D. Gupta*, E. Khan, Y. Blumenfeld
Institut de Physique Nucleaire, IN2P3-CNRS, Universite de Paris-Sud, 91406 Orsay Cedex, France
(Dated: February 9, 2008)

The elastic and inelastic proton scattering on ^{18,20,22}O nuclei are studied in a folding model formalism of nucleon-nucleus optical potential and inelastic form factor. The DDM3Y effective interaction is used and the ground state densities are obtained in continuum Skyrme-HFB approach. A semi-microscopic approach of collective form factors is done to extract the deformation parameters from inelastic scattering analysis while the microscopic approach uses the continuum QRPA form factors. Implications of the values of the deformation parameters, neutron and proton transition moments for the nuclei are discussed. The p-analyzing powers on ^{18,20,22}O nuclei are also predicted in the same framework.

Keywords: Elastic and Inelastic Proton Scattering; Analyzing Power; Effective Interaction; Folding Model; DDM3Y; HFB; QRPA
PACS numbers: 25.40.Cm, 25.40.Ep, 21.30.Fe, 25.60.-t

I. INTRODUCTION

The study of the oxygen isotopic chain deserves special attention since the neutron drip line was shown to be located at A = 24 [1, 2]. Thus rapid structural changes are expected as we move from ^{16}O towards its neutron-rich exotic isotopes. Several theoretical and experimental endeavors also indicate N = 14 and N = 16 shell closures [3]. In addition, there is opportunity to track neutron and proton contributions of the 2^+ state as the neutron drip line is approached [4]. Proton scattering is widely used as a means to study both macroscopic and microscopic aspects of nuclear structure [5, 6, 7, 8]. A suitable realistic effective nucleon-nucleon (NN) interaction is also needed in the analysis [6]. A folding model approach is followed in this study of proton scattering from ^{18,20,22}O at 43, 43, 46.6A MeV respectively, measured at GANIL [3, 9]. The earlier p-^{18}O differential cross section and analyzing powers for the ground state and 2^+_1 level at 24.5A MeV incident energy [10] are also included in the analysis. The folding model, which relates the density profile of the nucleus with the scattering cross sections is powerful tool for analyzing nucleus-nucleus scattering data at a few tens of MeV/nucleon [3, 6, 7, 8, 9, 10, 11, 12, 13]. Thus it is very appropriate for studying nuclei with extended density distributions. It should be noted that the same formalism is being followed to provide description of radioactivity, α and heavy ion scattering in a double folding model as well as nuclear matter and p-elastic/inelastic scattering in a single folding model [6, 14]

II. THEORETICAL FORMULATION

In a single folding calculation the nucleon-nucleus potential is obtained by using the density distribution of the nucleus and the nucleon-nucleon effective interaction [15] as,

$$U(\vec{r_1}) = \int \rho_2(\vec{r_2}) v(|\vec{r_1} - \vec{r_2}|) d^3\vec{r_2} \tag{1}$$

where $\rho_2(\vec{r_2})$ is density of the nucleus at $\vec{r_2}$ and $v(r)$ is the effective interaction between two nucleons at the sites $\vec{r_1}$ and $\vec{r_2}$. The finite range M3Y effective interaction $v(r)$ [16], is based upon a realistic G-matrix and was constructed in an oscillator basis. Effectively it is an average over a range of nuclear densities as well as energies and thereby has no explicit dependence on density or energy. The only rather weak energy dependent effect is contained in an approximate treatment of single-nucleon knock-on exchange. At lower energies, the density and energy averages are adequate for the real part of the heavy ion optical potentials. For scattering at higher energies, explicit density dependence was introduced [17, 18]. The present calculations use this density dependent M3Y (DDM3Y) effective NN interaction with an added zero-range pseudo potential given by,

$$v(r, \rho, E) = t^{\mathrm{M3Y}}(r, E) g(\rho, E) \tag{2}$$

* E-mail:dhruba@ipno.in2p3.fr

where E is incident energy and

$$t^{\rm M3Y} = 7999\frac{e^{-4r}}{4r} - 2134\frac{e^{-2.5r}}{2.5r} + J_{00}(E)\delta(r) \tag{3}$$

The zero-range pseudo-potential [17] represents the single-nucleon exchange term and is given by

$$J_{00}(E) = -276(1 - 0.005E/A){\rm MeV.fm}^3 \tag{4}$$

while the density dependent part is taken to be [18]

$$g(\rho, E) = c(1 - b(E)\rho^{2/3}) \tag{5}$$

taking care of the higher order exchange and Pauli blocking effects. Here $\rho = \rho_2$ is the spherical ground state density of the nucleus. The constants of this interaction c and b when used in single folding model description, are determined by nuclear matter calculations [14] as 2.07 and 1.62 fm^2 respectively.

III. CALCULATION AND ANALYSIS

The neutron and proton matter densities were calculated in the continuum Skyrme-Hartree-Fock-Bogoliubov (HFB) approach and the microscopic transition densities were obtained within the framework of the continuum QRPA (quasiparticle random phase approximation) formalism [3, 9, 19]. Fig. 1 shows the HFB ground state densities and QRPA transition densities for the 2^+_1 states of ^{18,20,22}O. In both HFB and QRPA calculations, all quasiparticle states below 60 MeV are considered, allowing to take into account seven oscillator shells.

In the present analysis both the real (V) and volume imaginary (W) parts of the folded nuclear potentials are assumed to have the same shape [6], i.e. $V_{\rm micro}(r) = V + iW = (N_{\rm R} + iN_{\rm I})U(r_1)$ where, $N_{\rm R}$ and $N_{\rm I}$ are the renormalization factors for real and imaginary parts respectively, obtained by fitting the elastic scattering data. In addition to real and volume imaginary folded potentials, best fit phenomenological surface imaginary and spin-orbit potentials ($4W_D$= 23.08, r_I= 1.17, a_I= 0.69, $4V_{s.o}$= 23.60, $r_{s.o}$= 0.88, $a_{s.o}$= 0.63) are also used as in [6]. The parameters are same for all targets, with volume integral per nucleon of the surface imaginary potential for ^{18,20,22}O as 176.5, 168.8 and 162.2 MeV fm^2 respectively. In [9], the first diffraction minimum of the elastic scattering on ^{20}O around $\theta_{\rm cm} = 35^o$ shows a discrepancy of about 50% with both phenomenological and microscopic calculations. It was thought that improvement of the imaginary part of the optical potential is required for these unstable nuclei. The more recent work [8] as well as the present formalism using a DDM3Y interaction satisfactorily explains the data.

The nucleon-nucleus optical potentials from elastic scattering best fits are subsequently used to generate the distorted waves for inelastic scattering amplitude calculations in DWBA formalism (Fig. 2). The calculations are performed using the code DWUCK4 [20]. Initially, the conventional approach of collective vibrational model ($\beta\frac{dV}{dr}$) is used to obtain the transition form factors. The deformation parameters β are determined by fitting the inelastic scattering angular distributions. Table 1 gives the renormalization factors, β values, χ^2/N for the folding model analysis. Compared to earlier results [9], the present β value of 0.33 for ^{18}O 2^+_1 agrees well while giving a slightly lower value of 0.46 for ^{20}O 2^+_1 state. The high β value of 0.50 for ^{20}O 2^+_1 state was explained [4] as neutrons playing a disproportionately large role in the excitation. The present calculations give the lowest β value of 0.26 for ^{22}O.

A more microscopic approach is useful to investigate low-lying excitations in exotic nuclei [3]. Calculations have also been performed (Fig. 2) with form factors using QRPA transition densities. It may be noted that two probes namely (p,p') and $B(E2)$ are required to derive proton and neutron contributions. The adopted values [21] for the reduced quadrupole transition rate $B(E2)$ from the ground state to 2^+_1 state for ^{18,20,22}O are used in this work and given in Table 2. Though the energy of the 2^+_1 state in ^{20}O is lower than ^{18}O, the $B(E2)$ value is considerably lower indicating a lesser degree of collectivity for ^{20}O [22].

In this context, the neutron/proton matrix element is defined as, $M_{n,p} = \int \delta\rho^{(\nu)}_{n,p}(r)r^{l+2}dr$, $\delta\rho^{(\nu)}_{n,p}(r)$ is the neutron (proton) transition density between ground state and excited state $|\nu>$ and $B(E2) = M_p^2$. As in [23], the proton transition density is first normalized (if required) to match with the experimental $B(E2)$ value. Then the magnitude of the neutron transition density is adjusted to give best fits to the inelastic scattering data. In an earlier folding model approach [8] substantially high values of M_n/M_p of 1.80 and 4.25 for ^{18}O and ^{20}O respectively were reported. The results of the present work are shown in Table 2 along with experimental M_n/M_p value [3, 9]. Though the $B(E2)$ value is lower, the present results on M_n/M_p of ^{20}O confirms its strong neutron contribution. Thus, for both ^{18}O

Table 1:
Renormalizations of DDM3Y folded potentials for p + ^{18,20,22}O scattering at incident energy (E/A) and excited state energy (E^*) in MeV, angular momentum transfer (l), deformation parameter (β), volume integral (J/A) of the real folded potential in MeV fm^3 and χ^2/N values from best-fits to the elastic and inelastic scattering data

Nucleus	E/A	E^*	$N_{\rm R}$	$N_{\rm I}$	l	β	$\chi^2_{\rm el}$/N	$\chi^2_{\rm inel}$/N	J/A
^{18}O*	43.0	1.98	0.90	0.08	2	0.33	7.55	0.81	-470.3
^{20}O*	43.0	1.67	0.88	0.08	2	0.46	2.04	2.15	-457.6
^{22}O*	46.6	3.17	0.73	0.08	2	0.26	5.05	4.61	-371.8

Table 2:
Reduced electric quadrupole transition probability $B(E2)$ in e^{2}fm^4, ratio of neutron to proton transition moment M_n/M_p. The proton part of the QRPA transition density was scaled to give experimental transition probability, while the neutron part was adjusted by the best fit to the inelastic scattering data

Nucleus	N/Z	E^*	$B(E2)$	E/A	$\chi^2_{\rm inel}$/N	$(M_n/M_p)_{expt}$	M_n/M_p	$(M_n/M_p)/(N/Z)$
^{18}O*	1.25	1.98	45.1±2.0	43.0	2.56	1.10±0.24	1.12	0.90
^{20}O*	1.50	1.67	28.1±2.0	43.0	6.59	3.25±0.80	3.34	2.23
^{22}O*	1.75	3.17	21.0±8.0	46.6	0.60	2.50±1.00	2.00	1.14

and ^{22}O the M_n/M_p ($0^+ \rightarrow 2^+$) values of 1.12 and 2.00 are close to the N/Z (N and Z are the neutron and proton numbers) values of 1.25 and 1.75 while for ^{20}O the M_n/M_p ($0^+ \rightarrow 2^+$) value of 3.34 is high as compared to the N/Z value of 1.50.

In Fig. 3, the elastic cross sections for p + ^{18,20,22}O scattering have been plotted as ratios to the Rutherford cross sections (scaled by a factor of 10 for clarity). Using the code CHUCK3 [20], the coupled channel (CC) calculations of the inelastic scattering cross sections are also shown in Fig 3. Only ground state and the first excited state have been considered and coupling is both ways. The DWBA and CC calculations using same form factors are nearly identical as can also be ascertained by the moderately high values of $N_{\rm R}$ from elastic scattering. Using different collective form factors give slightly different results. The dotted lines in Fig. 3 correspond to CC calculations using present collective form factors. The dashed lines in Fig. 3 correspond to form factors obtained from Legendre expansion of volume and surface Wood-Saxon potential, where monopole part of the potential is extracted.

It may be noted that the spin-orbit coupling in the present study is treated phenomenologically from the best fit optical potential parameters, since a phenomenological Thomas form for the spin-orbit potential gives a good description of the elastic data while the target excitation is simply represented by a nuclear transition density. The central transition potential explains the inelastic cross section reasonably well, giving a dominant contribution while the transition spin-orbit potential has only a minor effect [24]. The vector analyzing powers for ^{18}O(p,p') scattering at E= 24.5A MeV [10] are also compared with the calculations and the results are shown in Fig. 4. The Fig. 5 gives the predictions of analyzing powers for proton scattering from ^{18,20,22}O nuclei at 43, 43 and 46.6A MeV respectively, both for the ground state as well as the 2^+_1 excited states. The calculations are done on the same footing as the cross sections with HFB and QRPA approaches. For the ground state, while the 43A MeV p + ^{18,20}O angular distributions are nearly same, the p + ^{22}O analyzing power at slightly different energy of 46.6A MeV is marginally different. For the excited state all of them are nearly identical. It would indeed be interesting to observe how well the calculations agree with any future experimental data on p + ^{18,20,22}O analyzing powers.

IV. CONCLUSION

In this work, a single folding model approach is followed to study the cross sections as well as analyzing powers of proton scattering from neutron rich oxygen isotopes. In the DWBA formalism, both collective-model (deforming the optical potential) as well as microscopic calculations using HFB and QRPA densities with the DDM3Y effective interaction are carried out. The present calculations satisfactorily reproduce the experimental data showing a high neutron contribution to the excited state and a large β value for ^{20}O as compared to ^{18,22}O. Coupled channel calculations of the inelastic scattering cross sections reflect insignificant coupling. Predictions of the analyzing powers for ground state and excited state for proton scattering on the Oxygen isotopes at the same energies are given. With the availability of a larger data set on unstable nuclei, similar microscopic studies would be immensely helpful for nuclear structure and reaction studies.

[1] O. Tarasov et al.,Phys. Lett. B 409 (1997) 64
[2] H. Sakurai et al.,Phys. Lett. B 448 (1999) 180
[3] E. Becheva et al., Phys. Rev. Lett. 96 (2006) 012501; see references therein
[4] J.K. Jewell et al.,Phys. Lett. B 454 (1999) 181
[5] K. Amos, P. J. Dortmans, H. V. von Geramb, S. Karataglidis, Adv. in Nucl. Phys. 25 (2000) 275
[6] D. Gupta, D.N. Basu, Nucl. Phys. A 748 (2005) 402; see references therein
[7] D. Gupta, C. Samanta, Jour. Phys. G: Nucl. Part. Phys. 28 (2002) 85
[8] D. T. Khoa, Phys. Rev. C 68 (2003) 011601(R)
[9] E. Khan et al., Phys. Lett. B 490 (2000) 45
[10] J. L. Escudie, R. Lombard, M. Pignanelli, F. Resmini and A. Tarrats, Phys. Rev. C 10 (1974), 1645
[11] D. Gupta, C. Samanta, R. Kanungo, Nucl. Phys. A 674 (2000) 77
[12] H. Rebel, G. Hauser, G. W. Schweimer, G. Nowicki, W. Wiesner and D. Hartmann, Nucl. Phys. A 218 (1974) 13
[13] F. Petrovich, S. K. Yoon, M. J. Threapleton, R. J. Philpott, J. A. Carr, Nucl. Phys. A 563 (1993) 387
[14] D. N. Basu, Jour. Phys. G: Nucl. Part. Phys. 30 (2004) B7
[15] G. R. Satchler and W. G. Love, Phys. Rep. 55 (1979) 183
[16] G. Bertsch, J. Borysowicz, H. McManus and W.G. Love, Nucl. Phys. A 284 (1977) 399
[17] A.M. Kobos, B.A. Brown, R. Lindsay and G.R. Satchler, Nucl. Phys. A 425 (1984) 205
[18] A.K. Chaudhuri, Nucl. Phys. A 449 (1986) 243
[19] E. Khan, N. Sandulescu, M. Grasso, N. Van Giai, Phys. Rev. C 66 (2002) 024309
[20] P. D. Kunz, DWUCK4, CHUCK3 documentation available online at http://spot.colorado.edu/~kunz/DWBA.html
[21] S. Raman, C.W. Nestor Jr. and P. Tikkanen, Atomic Data and Nuclear Data Tables 78 (2001) 1
[22] P. G. Thirolf et al., Phys. Lett. B 485 (2000) 16
[23] E. Khan et al., Nucl. Phys. A 694 (2001) 103
[24] D. T. Khoa et al, Nucl. Phys. A 706 (2002) 61

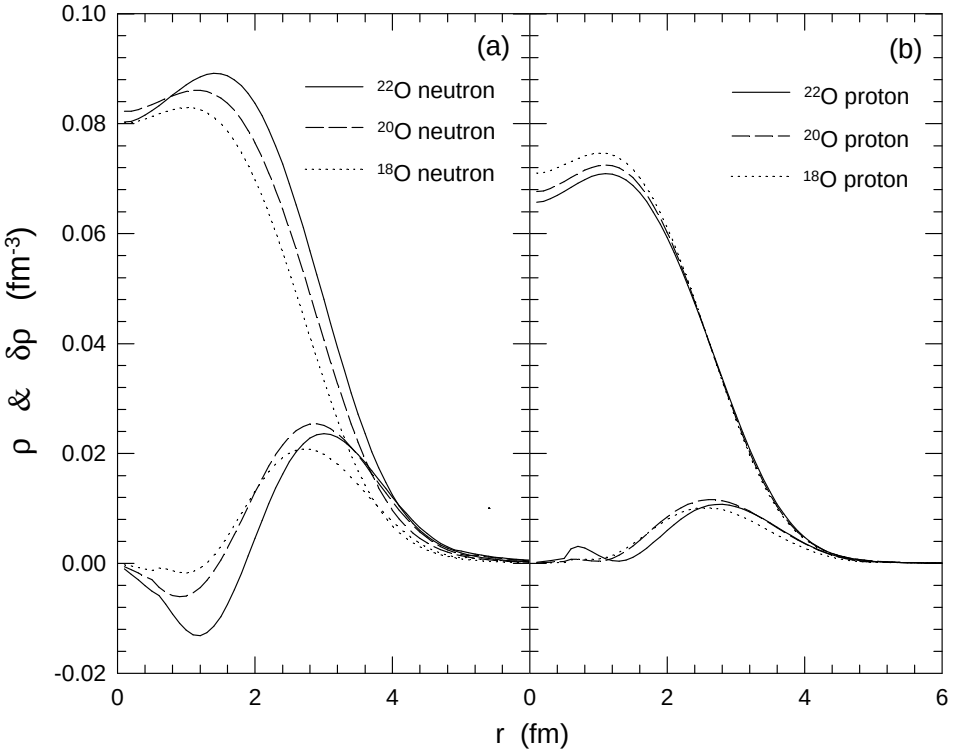

FIG. 1: (a) Neutron ground state densities (continuum Skyrme-HFB) and neutron transition densities (QRPA) for the 2_1^+ states of ^{18,20,22}O, (b) same as (a) but for protons

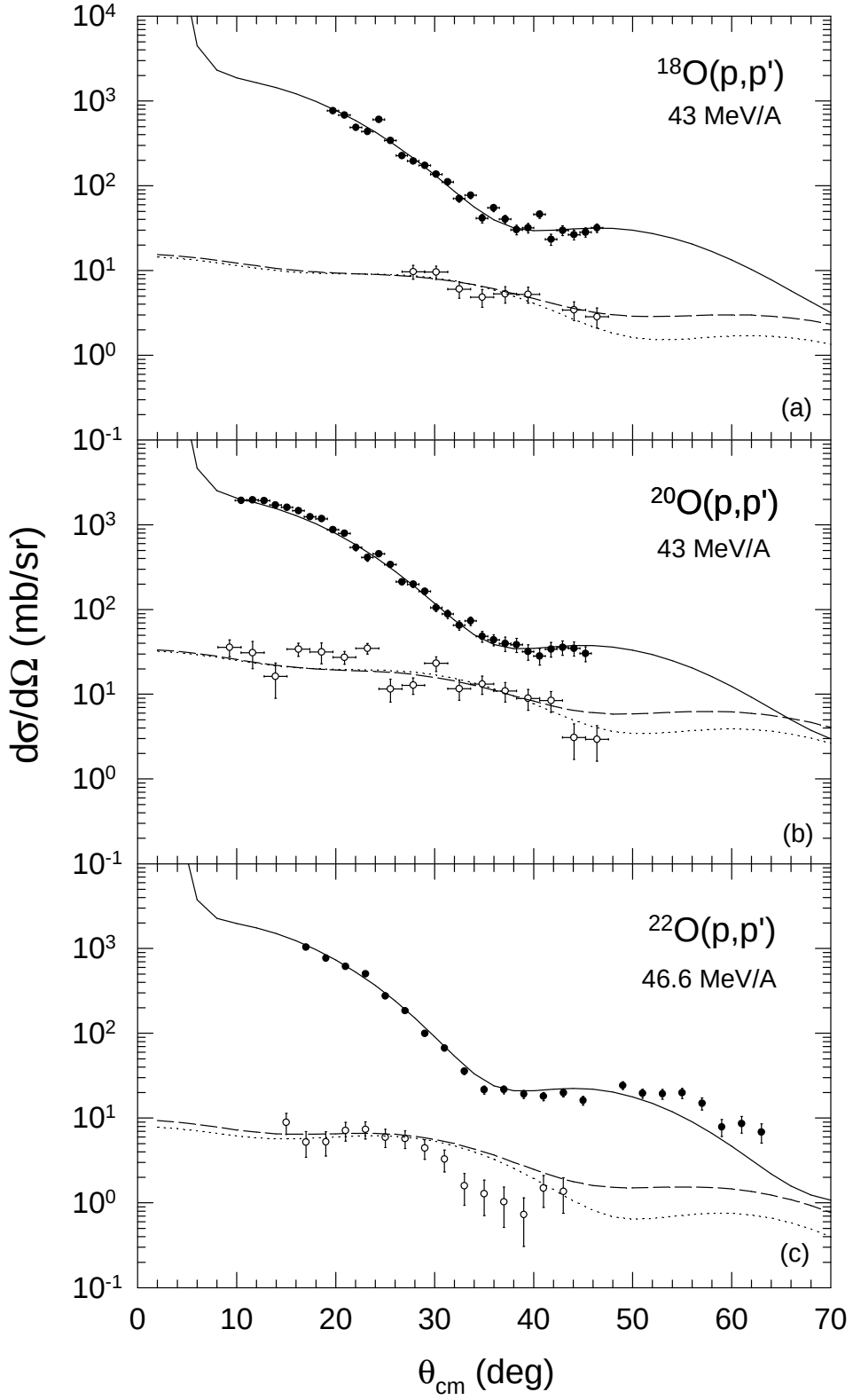

FIG. 2: The experimental angular distributions and folding model calculations of (a) p + ^{18}O at 43A MeV for elastic and inelastic [E^* = 1.98 MeV (2^+)] scattering [9], (b) p + ^{20}O at 43A MeV for elastic and inelastic [E^* = 1.67 MeV (2^+)] scattering [9], (c) p + ^{22}O at 46.6A MeV for elastic and inelastic [E^* = 3.17 MeV (2^+)] scattering [3]. The corresponding $N_{\rm R}$, $N_{\rm I}$ values are given in Table 1. The continuous, dashed (QRPA), dotted (collective) lines correspond to calculations for elastic and inelastic cross sections respectively.

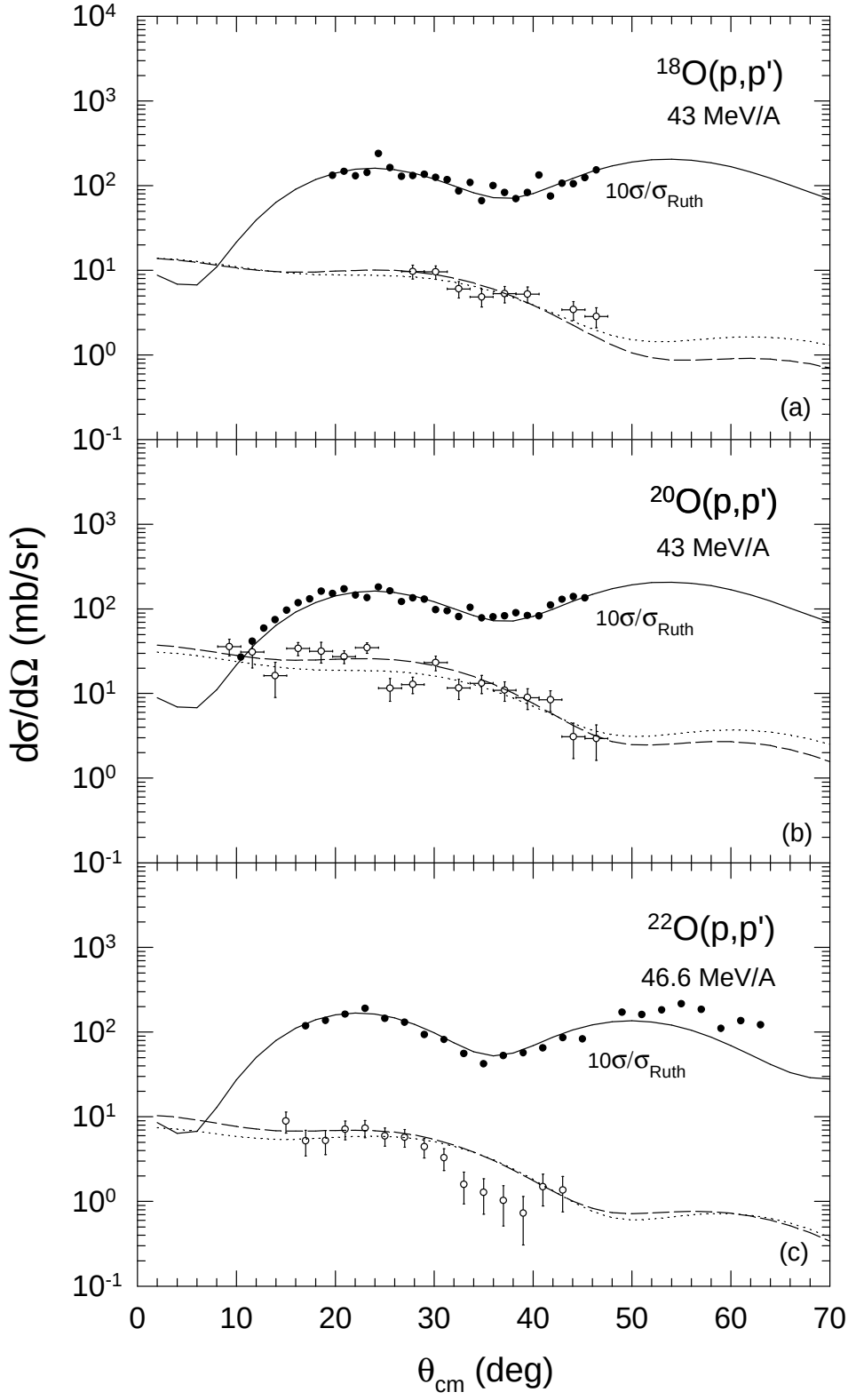

FIG. 3: Same as Fig. 2 but elastic cross sections are plotted as ratio to Rutherford cross sections (scaled by a factor of 10 for clarity). The dashed (Legendre expansion method) and dotted (deformed optical potentials) lines correspond to coupled channel calculations of the inelastic cross sections using two different collective form factors.

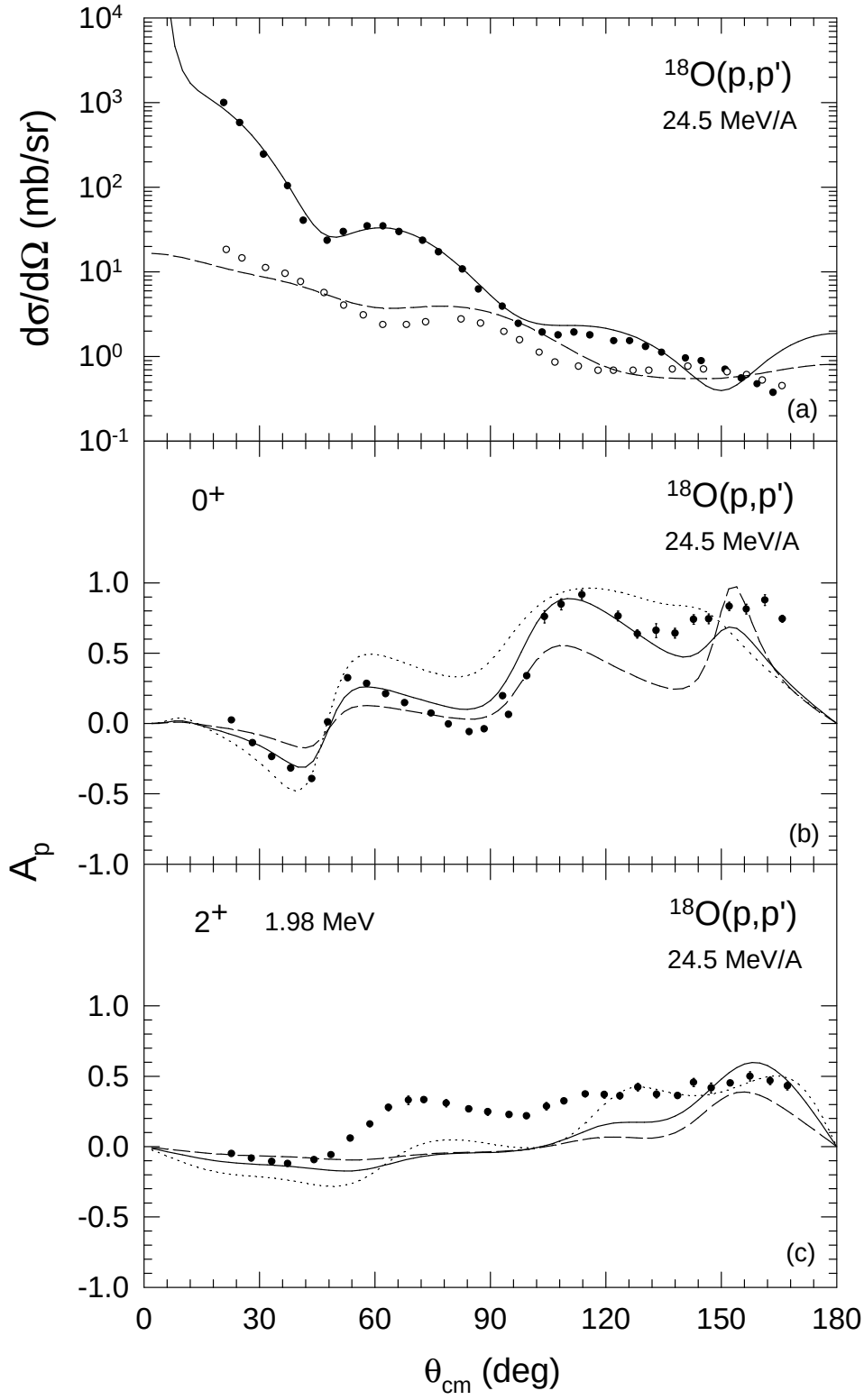

FIG. 4: The experimental angular distributions and folding model calculations of p + ^{18}O at 24.5A MeV [10] for (a) elastic and inelastic [$E^* = 1.98$ MeV (2^+)] differential cross section, (b) analyzing power for the ground state, (c) analyzing power for the excited state [$E^* = 1.98$ MeV (2^+)]. The QRPA transition densities are used in the calculations. In (b) and (c) the continuous, dashed and dotted lines correspond to calculations for 1.0, 0.5 and 2.0 times the spin-orbit term respectively.

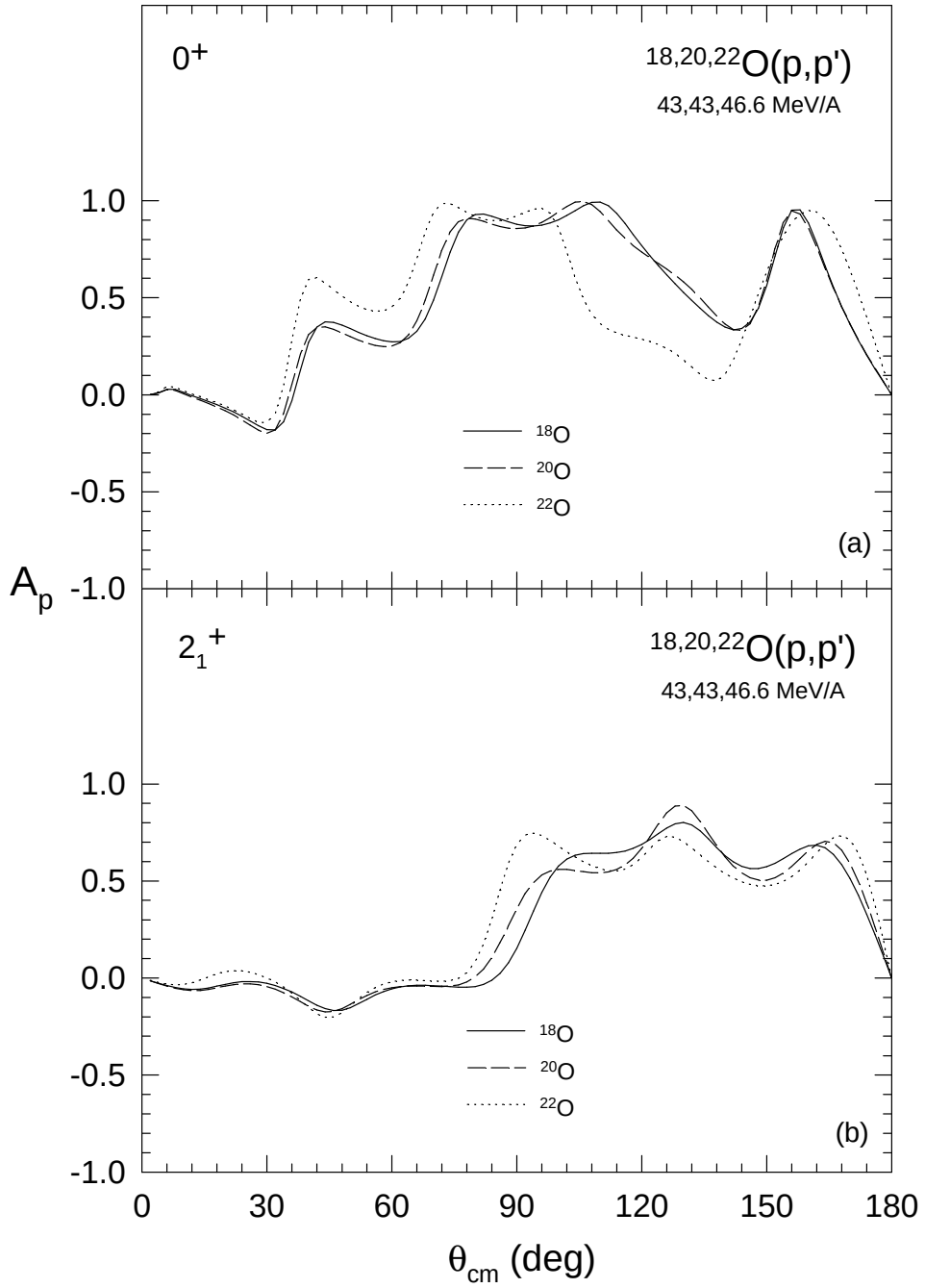

FIG. 5: The folding model calculations of p + ^{18}O at 43A MeV [E^* = 1.98 MeV (2^+)], p + ^{20}O at 43A MeV [E^* = 1.67 MeV (2^+)], p + ^{22}O at 46.6A MeV [E^* = 3.17 MeV (2^+)] for (a) analyzing power for the ground state, (b) analyzing power for the excited state. The QRPA transition densities are used in the calculations.